OPEN ACCESS

KING'S College LONDON

King's Research Portal

DOI:
10.1109/NSSMIC.2016.8069446

Document Version
Peer reviewed version

Link to publication record in King's Research Portal

Citation for published version (APA):
Mehranian, A., & Reader, A. J. (Accepted/In press). Multi-parametric MRI-guided PET image reconstruction. In *Nuclear Science Symposium and Medical Imaging Conference (NSS/MIC)* [8069446]
https://doi.org/10.1109/NSSMIC.2016.8069446

Citing this paper
Please note that where the full-text provided on King's Research Portal is the Author Accepted Manuscript or Post-Print version this may differ from the final Published version. If citing, it is advised that you check and use the publisher's definitive version for pagination, volume/issue, and date of publication details. And where the final published version is provided on the Research Portal, if citing you are again advised to check the publisher's website for any subsequent corrections.

General rights
Copyright and moral rights for the publications made accessible in the Research Portal are retained by the authors and/or other copyright owners and it is a condition of accessing publications that users recognize and abide by the legal requirements associated with these rights.

•Users may download and print one copy of any publication from the Research Portal for the purpose of private study or research.
•You may not further distribute the material or use it for any profit-making activity or commercial gain
•You may freely distribute the URL identifying the publication in the Research Portal

Take down policy
If you believe that this document breaches copyright please contact librarypure@kcl.ac.uk providing details, and we will remove access to the work immediately and investigate your claim.

Download date: 04. May. 2023

Multi-parametric MR-guided PET image reconstruction

Abolfazl Mehranian† and Andrew J. Reader

***Abstract*– In this study, we investigated the utilization of multi-contrast MRI as well as PET information to guide PET image reconstruction with the aim of addressing the pitfalls of conventional MR-guided PET image reconstruction methods. We studied the conventional Tikhonov and total variation (TV) priors, and the anatomical priors such as Kaipio, non-local Tikhonov with Gaussian and Bowsher similarity kernels and a local joint Burg entropy together with their extended multi-parametric versions. Our simulation results showed that joint Burg entropy far outperforms the conventional anatomical priors in the preservation of PET unique lesions and in the reconstruction of functional boundaries with matched MR anatomical boundaries. It was found that the multi-parametric extension of the priors leads to enhanced preservation of edge and PET unique features. The clinical reconstructions showed that the Gaussian similarity kernels with voxel-based feature vectors, the Bowsher method and the Burg prior are the best performing priors and their multi-parametric extensions led to the improved recovery of the PET unique features.**

Index Terms – PET-MRI, Bowsher, Total variation, joint entropy

I. Introduction

Simultaneous PET-MR systems provide complementary multi-parametric MRI information for PET imaging which can be exploited during PET image reconstruction to reduce noise and partial volume effect (PVE). The Bayesian maximum a posteriori (MAP) image reconstruction has been mainly explored to exploit the *a priori* knowledge of the unknown image obtained from the anatomical images. Over the last two decades, various anatomical priors have been designed to improve upon the conventional quadratic prior using edge preserving potential functions that assign a lower penalty to large local differences on the assumption that they are probably associated with valid boundaries. Bowsher *et al* [1] proposed to perform smoothing between the PET image voxels that their corresponding MR image voxels are anatomically similar, according to their absolute intensity differences. This anatomically guided quadratic prior essentially weights the local differences using zero-one weighting factors, thereby disabling the smoothing across boundaries, but encouraging it within anatomical regions. The main concern with such anatomical priors is the mismatched between PET and MR images, which can lead to suppression of true PET features or introduction of false ones. Inspired by non-local means filtering, Chen *et al* [2] proposed the calculation of similarity weighting factors from the current PET images estimate using patch-based Gaussian kernels. To improve the performance of the Bowsher prior in the case of the anato-functional inconsistencies, Kazantsev *et al* [3] investigated the combination of the Bowsher and Chen methods. Another approach is to improve MRF priors using the normalized gradient vector fields (normal vectors) obtained from anatomical side information. More recently, Ehrhardt *et al* [4] derived a prior based on the structural similarity of the PET and MR images measured by the alignment of the PET and MR gradients. In fact, this prior generalizes the prior proposed by Kaipio *et al* [5] for improving the quadratic prior by weighting the magnitude of PET image gradients (i.e. local differences) with the sin-squared angle between the PET gradients and MR normal vectors. The Shannon joint entropy (JE) has also been studied as an anato-functional prior able to cope with PET-MR mismatches as it relies on their joint probability distribution; however, it also ignores the spatial correlation between neighbouring voxels, which is an important feature for PET tracers that are confined in anatomical regions. Vunckx *et al* [6] showed that the Bowsher prior overall outperforms this JE prior as it has less hyper-parameters and it does not converge to an undesirable local maximum.

The availability of multi-parametric images in simultaneous PET-MR systems can provide a unique opportunity for improving PET image quality. These parametric maps are mutually complementary and informative, for instance, an early-stage lesion might not have any morphological manifestations in T1- or T2-weighted MR images but might appear metabolically active in PET images. The aim of this study is to explore this promising aspect of simultaneous PET-MR imaging. Specifically, we **a)** elaborate different priors included the Tikhonov (quadratic) and total variations (TV) priors (as local regularization methods), the non-local Tikhonov and Bowsher priors (as non-local anatomically guided regularization methods), the Kaipio prior and a local Burg joint entropy prior modified to include the spatial correlation between neighbouring voxels. Further, we **b)** test their performance using realistic 3D simulations and clinical datasets, and finally **c)** generalize the amenable priors to multi-parametric MR-guided PET image reconstruction, where the complementary MR images as well as the PET image itself are used to improve the PET image quality data.

II. Material and Methods

A. Maximum a posteriori PET image reconstruction

Let $\boldsymbol{y} \in \mathbb{Z}_+^M$ the PET data scan of an object with the activity distribution represented by $\boldsymbol{u} \in \mathbb{R}^N$. The MAP reconstruction consists of maximizing the posterior probability of $\boldsymbol{u}$ given $\boldsymbol{y}$, that is:

$$\widehat{\boldsymbol{u}} = \underset{\boldsymbol{u}}{\operatorname{argmax}} \left\{ \sum_{i=1}^{M} [\boldsymbol{G}\boldsymbol{u}]_i + \bar{r}_i - y_i log_e([\boldsymbol{G}\boldsymbol{u}]_i + \bar{r}_i) - \beta R(\boldsymbol{u}) \right\} \quad (1)$$

where g_{ij} is the geometric probability detection of annihilation events emitted from the jth voxel in the ith PET detector and $\bar{r}_i$ is the expected number of scatter and random events in the ith detector. In this study, we considered the following prior, which generalizes most of the included MRF priors:

$$R(\boldsymbol{u}) = \sum_j^N \phi\left(\sum_{b \in \mathcal{N}_j} \xi_{jb}\omega_{jb}\psi(u_j - u_b) \right) \quad (2)$$

ψ and ϕ are potential functions, where ψ operates on the intensity differences between the jth voxel and its neighbouring voxels, and ϕ operates on the neighbourhood $\mathcal{N}_j$ sum of those local differences. ξ_{bj} and ω_{bj} are coefficients that weight the intensity differences between voxels j and b based on their proximity (e.g. the inverse of their Euclidean distance) and based on their similarity, respectively. The Tikhonov prior is defined by setting $\psi(s) = s^2$ and $\phi(t) = t$, while the smoothed isotropic TV prior is defined for $\psi(s) = s^2$ and $\phi(t) = \sqrt{t + \delta^2}$, where $\delta > 0$ is a smoothing factor.

The similarity weighting coefficients (kernels) encourage the smoothness along boundaries but discourage it across them. General-

A. Mehranian and A. J. Reader are with Division of Imaging Sciences and Biomedical Engineering, Department of Biomedical Engineering, King's College London, St. Thomas' Hospital, London, UK. †Email: Abolfazl.Mehranian@kcl.ac.uk.

ly, there are three approaches in the calculation of these coefficients, based on: i) the PET image reconstructed from a previous iteration [2] ii) the MRI or CT side anatomical information as in the Bowsher method and iii) both the PET and side anatomical information [3, 7]. In this study, we extend the latter to multi-parametric MRI and PET, where the similarity kernels are calculated based on all available MRI data as well as the PET image.

1) Bowsher and Gaussian similarity kernels

In Bowsher method, the top B most similar neighbours in the MR image is declared similar in their corresponding PET images based on their absolute differences. The similarity weights can also be calculated based on Gaussian kernels as a function of a reference image $\boldsymbol{x}$:

$$\omega_{jb}^{Voxel}(\boldsymbol{x}) = \exp\left(-\frac{(x_j - x_b)^2}{2\sigma^2}\right),\ \ \omega_{jb}^{Patch}(\boldsymbol{x}) = \exp\left(-\frac{\|\boldsymbol{f}_j(\boldsymbol{x}) - \boldsymbol{f}_b(\boldsymbol{x})\|_2^2}{2\sigma^2}\right) \quad (3)$$

where ω_{bj}^{Voxel} and ω_{bj}^{Patch} are the kernels with voxel-based and patch-based feature vectors, $\boldsymbol{f}_l(\boldsymbol{x}) \in \mathbb{R}^L$ is a vector of L voxel values on a patch centred on the lth voxel, known as a feature vector, σ is the shape parameter (standard deviation) of the Gaussian function. The inclusion of patch-based feature vectors ω_{jb}^{Patch} makes the similarity kernels robust to noise and random fluctuations. In this study, we defined a non-local multi-parametric similarity kernel as the geometric mean of the kernels calculated from the PET image, $\boldsymbol{u}$, and those calculated from the MR images, $\{\boldsymbol{v}^{(i)}\}$, as follows:

$$\omega_{jb} = \frac{1}{Z}\left(\omega_{jb}^{Patch}(\boldsymbol{u})\prod_{i=1}^{P}\widetilde{\omega}_{jb}(\boldsymbol{v}^{(i)})\right)^{1/(P+1)} \quad (4)$$

, let $\{\boldsymbol{v}^{(i)} \in \mathbb{R}^N\}_{i=1}^{P}$ be a set of P multi-parametric MR images where $\omega_{jb}^{Patch}(\boldsymbol{v})$ is a self-similarity Gaussian kernel with patch-based feature vectors, as in (3), and $\widetilde{\omega}_{jb}$ is side-similarity Bowsher kernel or Gaussian kernel voxel-based feature vectors. The derivative of the weighted quadratic prior is given by:

$$\frac{\partial R(\boldsymbol{u})}{\partial u_j} = 2\sum_{b\in\mathcal{N}_j}\xi_{jb}\omega_{jb}(u_j - u_b) \quad (5)$$

2) Kaipio prior

Based on the formulations in [4], the Kaipio prior is defined as:

$$R(\boldsymbol{u}) = \sum_j^N\sum_{b\in\mathcal{N}_j}\xi_{jb}(u_j - u_b)^2 - \left(\sum_{b\in\mathcal{N}_j} n_{jb}\sqrt{\xi_{jb}}(u_j - u_b)\right)^2 \quad (6)$$

$$n_{jb} = \frac{v_j - v_b}{\sqrt{\sum_{b\in\mathcal{N}_j}(v_j - v_b)^2}}$$

a quadratic prior improved by inclusion of the squared inner product of the PET image gradient and MR normal vectors $\boldsymbol{n}_j$. The derivative of the Kaipio prior is the same as in (5) with the weights given by:

$$\omega_{jb} = 1 - \frac{n_{jb}}{\sqrt{\xi_{jb}}}\sum_{b\in\mathcal{N}_j} n_{jb}\sqrt{\xi_{jb}} \quad (7)$$

3) Local joint Burg entropy

In this study, a multi-parametric joint entropy (JE) prior was defined based on the negative of the Burg entropy [8]:

$$H(\boldsymbol{U}, \boldsymbol{V}^{(1)}, \dots, \boldsymbol{V}^{(P)}) \approx -\sum_j^N \log p\left(u_j, v_j^{(1)}, \dots, v_j^{(P)}\right)$$

where the variables $\boldsymbol{u}, \boldsymbol{v}^{(1)}, \dots, \boldsymbol{v}^{(P)}$ are parametric PET and MRI images and $p(x, y, \dots, z)$ is the joint probability distribution (PDF) of the variables estimated using a multivariate Gaussian window function with a diagonal covariance matrix $\boldsymbol{\Sigma} = \mathrm{diag}\{\sigma_u^2, \sigma_{v^{(1)}}^2, \dots, \sigma_{v^{(P)}}^2\}$:

$$p(x, y, \dots, z) = \frac{1}{N}\sum_b^N \mathcal{G}(x, u_b, \sigma_u)\mathcal{G}\left(y, v_b^{(1)}, \sigma_{v^{(1)}}\right)\dots\mathcal{G}\left(z, v_b^{(P)}, \sigma_{v^{(P)}}\right) \quad (8)$$

$$\mathcal{G}(q, r, \sigma) = \frac{1}{\sqrt{2\pi}\sigma}\exp\left(-\frac{(q-r)^2}{2\sigma^2}\right)$$

where N is the number of samples used to calculate the PDF, which similar to [9] was set equal to the number of voxels in the images. The derivative of joint entropy evaluated at jth bin (or voxel) depends on all voxel intensities simultaneously, which leads to discarding regional information. As suggested in [9], the derivative can be approximated by evaluating the summation for the voxels that are in the neighbourhood of the jth voxel, that is:

$$\frac{\partial H}{\partial u_j} = 2\sum_{b\in\mathcal{N}_j}\xi_u\widehat{\omega}_{jb}(u_j - u_b), \qquad \xi_u = \frac{1}{2N\sigma_u^2} \quad (9)$$

where $\widehat{\omega}_{jb}$ act as similarity weighting coefficients given by:

$$\widehat{\omega}_{jb} = \frac{\exp\left(-\frac{(u_j - u_b)^2}{2\sigma^2}\right)\prod_{i=1}^{P}\exp\left(-\frac{\left(v_j^{(i)}, v_b^{(i)}\right)^2}{2\sigma_{v^{(i)}}^2}\right)}{p\left(u_j, v_j^{(1)}, \dots, v_j^{(P)}\right)} \quad (10)$$

To further improve this prior in spatial neighbourhoods, we replaced ξ_u in (9) with the proximity coefficients ξ_{jb} in (2).

B. Optimization and parameter selection

The MAP problem in (1) was optimized using the Green's one-step-late (OSL) MAP-EM algorithm, as follows:

$$u_j^{n+1} = \frac{u_j^n}{\sum_{i=1}^M g_{ij}n_i a_i + \beta\frac{\partial R(\boldsymbol{u}^n)}{\partial u_j}}\sum_{i=1}^{M} g_{ij}n_i a_i\frac{y_i}{n_i a_i\sum_b g_{ib}u_b^n + r_i} \quad (11)$$

The priors included in the present work have a number of user-defined parameters that determine their performance. Table 1 summarizes these key parameters, along with those with pre-defined values commonly used in our simulation and clinical data reconstructions.

TABLE 1 LIST OF THE PARAMETERS OF THE REGULARIZATION METHODS INCLUDED IN THIS STUDY. THE PRE-DEFINED VALUES OF SOME OF THE PARAMETERS COMMONLY USED IN THIS STUDY ARE ALSO PRESENTED.

PRIORS	PARAMETERS
Local Tikhonov	$\lvert\mathcal{N}_3\rvert = 6, \beta$
Local TV	$\lvert\mathcal{N}_3\rvert = 6, \delta = 1\times10^{-3}, \beta$
Kaipio	$\lvert\mathcal{N}_7\rvert = 342, \beta$
†Gaussian-V	$\lvert\mathcal{N}_7\rvert = 342, \sigma_u, \beta$
*Gaussian-P	$\lvert\mathcal{N}_7\rvert = 342, \lvert\mathcal{F}_3\rvert = 26, \sigma_u, \beta$
Bowsher	$\lvert\mathcal{N}_7\rvert = 70, \beta$
Joint Burg entropy	$\lvert\mathcal{N}_7\rvert = 342, \sigma_u, \sigma_v, \beta$

†,*Gaussian similarity kernels with voxel (V) and patch (P) based feature vectors.
$|\mathcal{N}_n|$, $|\mathcal{F}_n|$: number of included neighbors in a $n\times n\times n$ neighborhood ($\mathcal{N}$) or feature vector ($\mathcal{F}$)
β: Prior's weighting factor (regularization parameter)
δ: TV smoothness parameter
σ_u, σ_v: Standard deviation of Gaussian kernels used for PET and MR images
B: number of most similar neighboring voxels

C. Numerical PET-MR simulations and clinical datasets

The *BrainWeb* phantom [10] was utilized to simulate a 10 million counts ^{18}F-FDG scan in the brain for Siemens mMR scanner together with T1- and T2-weighted MR images and attenuation maps, all with a matrix size of 344×344×127 and voxel of size 2×2×2 mm^3. A few regions of the T1 and T2-MR images were uniquely and commonly removed in such a way that the anatomical inconsistencies were simulated. An [^{18}F]FDG PET scan was included with about 650 million prompts.

III. RESULTS

A. Simulations

Fig. 1 compares the reconstruction results of the brain phantom using the studied algorithms including: the MLEM algorithm with 4 mm Gaussian filtering, local Tikhonov and TV priors and T1-MR anatomical priors, i.e. the Kaipio, non-local Tikhonov with patch- and voxel-based Gaussian similarity kernels (Gaussian-P/V), Bowsher and the joint Burg entropy. As can be seen, the MAP reconstruction methods have substantially reduced noise and preserved matched PET-MR edges.

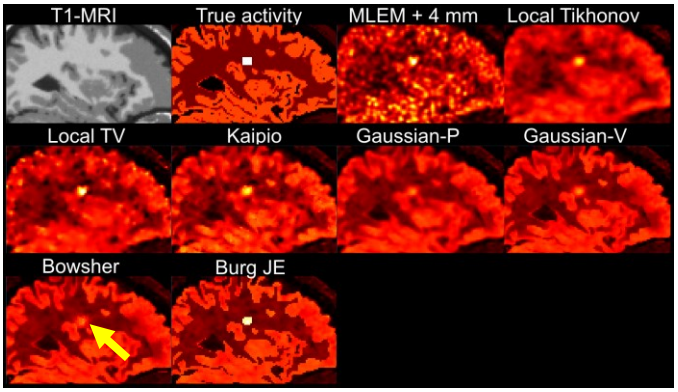

Fig. 1. The results of the MAP image reconstructions of the brain phantom using the conventional local and non-local anatomical priors, compared to the MLEM reconstruction followed by Gaussian filtering with kernel width of 4 mm.

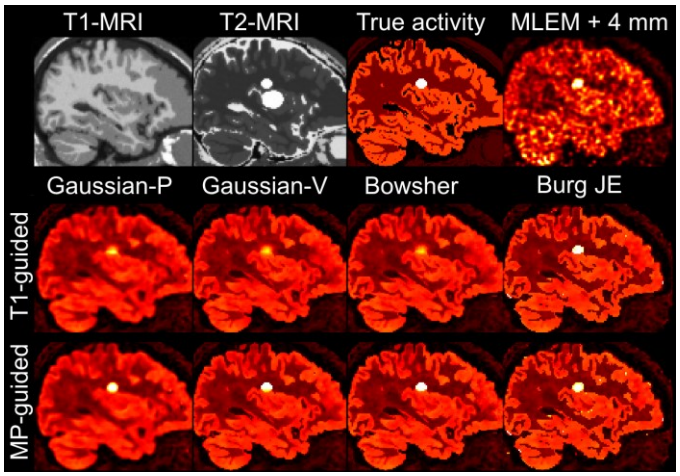

Fig. 2. The results of the MAP image reconstructions of the brain phantom using the T1-MR and multi-parametric (MP) MR guided anatomical priors. All PET images are shown with the same displaying window.

The results show that the Gaussian-V, Bowsher and Burg methods achieve the best performance for the region where the PET and MR image have common boundaries. However, as shown, it is noticeable that the Gaussian-P/V and Bowsher priors tend to completely suppress the PET-unique lesion compared to the Kaipio and JE priors. For PET regions that do not have corresponding MRI regions, the Kaipio degenerates to the Tikhonov prior, therefore for this simulated lesion, they perform similarly. On the other hand, the Burg prior in essence relies of both MRI and PET information, therefore it is able to preserve PET unique feature. The results show that by proper selection of the σ_u parameter, the Gaussian-V method can approach the Bowsher method with a given B number.

TABLE 2. THE NRMSE RESULTS OF THE RECONSTRUCTION METHODS IN THE BRAIN PHANTOM CONVENTIONAL T1-MR GUIDED ANATOMICAL PRIORS AND THE MULTI-PARAMETRIC (MP) GUIDED ANATOMICAL PRIORS (GM: GREY MATTER, WM: WHITE MATTER).

Methods	GM	WM	Tumours
MLEM	33.63	63.57	25.52
Local Tikhonov	27.49	55.98	26.93
Local TV	31.68	60.31	**23.43**
Kaipio	22.21	45.72	26.73
Gaussian-P	21.08	44.95	33.14
Gaussian-V	16.48	38.15	33.67
Bowsher	**13.17**	30.73	35.04
Burg JE	16.30	29.89	24.72
Gaussian-P: MP	20.77	43.57	30.42
Gaussian-V: MP	13.75	32.41	28.99
Bowsher: MP	**11.59**	**24.18**	28.70
Burg JE: MP	16.81	**24.60**	**24.70**

Table 1 presents the NRMSE results of the reconstruction methods calculated over GM, WM and tumours of the brain phantom. The results shows that in GM, the Bowsher gives rise to the lowest errors especially with its multi-parametric (MP) extension which compensates for the mismatches between PET and T1-MR images. In the WM of the simulated FDG phantom, where there is less uptake, both MP Bowsher and Burg JE prior outperform the other methods, whereas in the tumours, the TV and JE priors achieve the lowest errors. As can be seen, the Bowsher and Gaussian priors lead to the highest NRMSE in the tumours, which is consistent with findings in Fig. 1. The ability of the TV prior in preservation of the active tumours should be ascribed to the fact that for the voxels that the magnitude of their local differences is large, the prior assigns lower weights on those differences.

Fig. 2 show the results of MP guided PET image reconstructions in the brain phantom dataset for the Gaussian-P/V, Bowsher and Burg JE priors in comparison with T1-MR guided reconstructions. As shown, there are a missing tumour and a mismatched anatomical region that is partly complemented by the T2-MR image. In the T2-MR image however there are two lesions of which the smaller one matches the PET lesion. The results showed that the inclusion of T2-MR and as well as PET information can lead improved recovery of the lesion in the PET images. As can be seen, the large lesion in T2-MR image has not significantly induced false edges in the MP-guided PET images, however, in all reconstructions there are a faint trace of the inferior edge of the lesion especially in the JE prior, where noise has been sparely preserved. The NRMSE results in Table 3 also confirms the improved performance of the multi-parametric priors compared to the conventional anatomical priors

B. In-vivo evaluation

Fig. 3 compares the reconstruction results of the FDG brain dataset using MLEM, conventional MAP and anatomical MAP reconstructions using the T1-MPRAGE MR image and also shows the fused T1-MR and the PET images reconstructed by MLEM and Burg methods. The results demonstrate that the overall resolution and quality of PET images have been improved by inclusion of anatomical information, especially using the Gaussian-V, Bowsher and JE priors. As a result, the spill-over and partial volume averaging effects visible in the MLEM and Tikhonov and TV reconstructions have been considerably reduced by the anatomical priors.

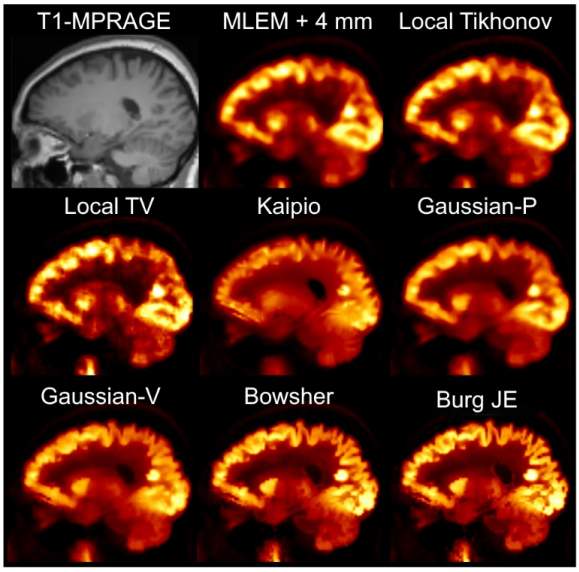

Fig. 3. The reconstruction results of the clinical FDG dataset. The activity profiles of the reconstruction methods has been shown for three different regions along the indicated dash lines.

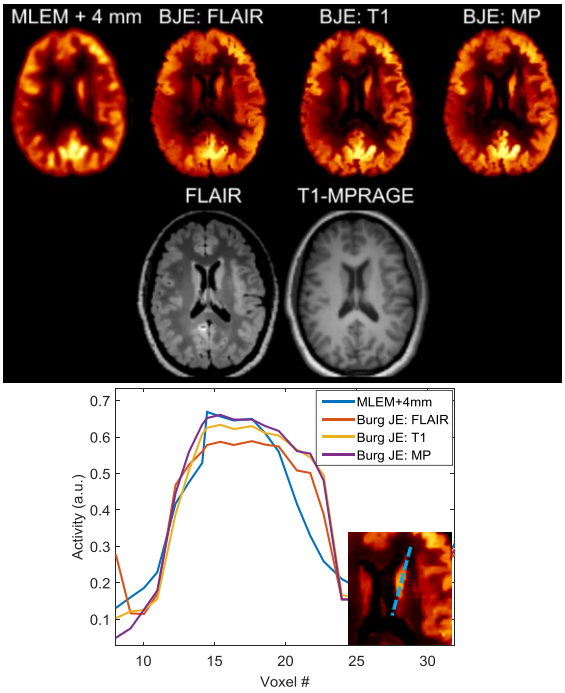

Fig. 4 The reconstruction results of the clinical FDG dataset using the proposed approximate joint entropy prior employing FLAIR, T1 MRI data and multi-parametric T1-FLAIR-PET (MP) data during reconstruction.

Fig. 4 compares the reconstruction results of the joint Burg entropy prior guided by FLAIR-MR, T1-MR image as well as all parametric images. The quality of the anatomically-guided PET image reconstructions highly depends on the quality and the amount of information provided by the MR images. The visual comparison of the reconstructions reveals there are subtle differences between the reconstruction, however, the activity profiles drawn along the head of caudate shows the FLAIR-guided JE method slightly underestimates the activity whereas its MP extension recovers the activity profile toward that of the MLEM method.

IV. Conclusion

In this work, several state-of the-art anatomical priors were studied and presented in a common framework as a non-local Tikhonov prior with different similarity weighing coefficients. In addition, we proposed the extension of the prior to multi-parametric MR-guided PET image reconstruction in which available complementary MRI and PET are exploited to improve the PET image quality and to address the pitfalls of the conventional MR-guided anatomical priors. The results showed that the Tikhonov prior with Gaussian similarity kernels, calculated using voxel-based feature vectors, the Bowsher similarity kernels and the local joint Burg entropy prior results in the most accurate recovery of PET details. It was also found that the Burg prior is more robust in preserving PET unique features, as by definition it relies on both PET and MRI information. In both our simulation and clinical results, the conventional anatomical prior resulted in the suppression of PET unique features, which was notably reduced by the multi-parametric extension of these priors.

Acknowledgements

This work is supported by Engineering and Physical Sciences Research Council (EPSRC) under grant EP/M020142/1.

References

[1] J. E. Bowsher, H. Yuan, L. W. Hedlund, T. G. Turkington, G. Akabani, A. Badea, *et al.*, "Using MRI information to estimate F18-FDG distributions in rat flank tumors," in *IEEE Nucl. Sci. Symp. Conf. Record*, 2004, pp. 2488-2492.

[2] Y. Chen, J. Ma, Q. Feng, L. Luo, P. Shi, and W. Chen, "Nonlocal Prior Bayesian Tomographic Reconstruction," *J Math Imaging Vis,* vol. 30, pp. 133-146, 2008.

[3] D. Kazantsev, A. Bousse, S. Pedemonte, S. R. Arridge, B. F. Hutton, and S. Ourselin, "Edge preserving bowsher prior with nonlocal weighting for 3D SPECT reconstruction," in *IEEE International Symposium on Biomedical Imaging*, 2011, pp. 1158-1161.

[4] M. Ehrhardt, P. Markiewicz, M. Liljeroth, A. Barnes, V. Kolehmainen, J. Duncan, *et al.*, "PET Reconstruction with an Anatomical MRI Prior using Parallel Level Sets," *IEEE Trans Med Imaging,* Apr 14 2016.

[5] J. P. Kaipio, V. Kolehmainen, M. Vauhkonen, and E. Somersalo, "Inverse Problems with Structural Prior Information," *Inverse Probl.,* vol. 15, pp. 713-729, 1999.

[6] K. Vunckx, A. Atre, K. Baete, A. Reilhac, C. M. Deroose, K. Van Laere, *et al.*, "Evaluation of three MRI-based anatomical priors for quantitative PET brain imaging," *IEEE Trans Med Imaging,* vol. 31, pp. 599-612, Mar 2012.

[7] V. G. Nguyen and S. J. Lee, "Incorporating anatomical side information into PET reconstruction using nonlocal regularization," *IEEE Trans Image Process,* vol. 22, pp. 3961-73, Oct 2013.

[8] C. L. Byrne, "Iterative image reconstruction algorithms based on cross-entropy minimization," *IEEE Trans Image Process,* vol. 2, pp. 96-103, 1993.

[9] S. Somayajula, C. Panagiotou, A. Rangarajan, Q. Li, S. R. Arridge, and R. M. Leahy, "PET image reconstruction using information theoretic anatomical priors," *IEEE Trans Med Imaging,* vol. 30, pp. 537-49, Mar 2011.

[10] C. A. Cocosco, V. Kollokian, R. K.-S. Kwan, and A. C. Evans, "BrainWeb: online interface to a 3D MRI simulated brain database," *NeuroImage,* vol. 5, p. S425, 1997.